

Unified Aerodynamic-Influence-Coefficient Approach for Aeroservoelastic and Multidisciplinary Optimization Applications

P. C. Chen* and D. Sarhaddi†

ZONA Technology, Inc., Scottsdale, Arizona 85251

D. D. Liu‡

Arizona State University, Tempe, Arizona 85287

and

M. Karpel§

Technion—Israel Institute of Technology, 32000 Haifa, Israel

A unified aerodynamic influence coefficient (UAIC) method has been developed for aeroservoelastic (ASE) analysis as well as multidisciplinary optimization (MDO) applications. The UAIC method is applicable to all Mach numbers from subsonic, to transonic, to supersonic, to hypersonic flight regimes. It is fully compatible with the structural finite element method and, hence, with an MDO system such as ASTROS. Based on this UAIC approach, a unified aerodynamic module ZAERO and an ASE module can be developed; the former performs in the k domain and the latter in the s domain. A minimum-state technique is found most effective in converting the k -domain solution to the s domain for all Mach numbers. Flutter results computed by the root-locus method are found to agree well with those of the V - g method and measured data.

Introduction

In recent years, rapid progress in aeroservoelasticity (ASE) and multidisciplinary optimization (MDO) has demanded further improvement of computational aerodynamic methods in their capability to generate s -domain aerodynamics, their compatibility with structural finite element methods (FEM), and their expediency for design optimization. Additionally, design variables such as wing thickness, body-wing configurations, and the full Mach number range to cover transonic and hypersonic flow regimes are considered important parameters to be included in a general aerodynamic module, ready to be integrated with an MDO system such as ASTROS.¹

Although current computational fluid dynamics (CFD) methods are gradually reaching a rather mature stage for steady aerodynamic design/analysis, their acceptance by industry for aeroelastic applications is still hampered by the problems in grid generation, CFD/computational structural dynamics (CSD) interfacing, and affordable computing time. For example, without a major modification, the program structure of ASTROS does not allow its interfacing with a time-accurate CFD method.^{2,3} On the other hand, panel methods imbedded in the Aero module of ASTROS such as the doublet-lattice method (DLM) and the constant pressure method (CPM), albeit fully compatible with the structural FEM, require further improvement in their robustness, their confinement to lifting surfaces (rather than wing-body systems), and their applicability to transonic and hypersonic Mach numbers.

Toward this end, during the last few years we have critically reexamined the cited lifting surface methods from the viewpoint of program robustness and range of applicability. The result of this reexamination is an effort to develop a unified aerodynamic influ-

ence coefficient (UAIC) approach extending the applicability of our current wing-body AIC methods from the linear flow regime^{4–6} to the transonic and hypersonic regimes.^{7–9}

On the other hand, ASE mandates the s -domain aerodynamics as a base, which can be obtained from the k -domain aerodynamics by means of several rational approximation methods.^{10–14} Among these methods, the minimum-state technique (MIST)^{13,14} is selected for its effectiveness and its readiness for MDO applications. Although much success has been claimed for MIST in dealing with the linear aerodynamics in the subsonic and supersonic regimes, its applicability to the unsteady aerodynamics in the transonic and hypersonic regimes remains to be established.

Our objective, therefore, is to present the development of a unified aerodynamic module (ZAERO) and an ASE module, both supported by the UAIC approach. The integration of both modules into an MDO environment such as ASTROS¹⁵ will be described.

Aeroservoelastics in State-Space Form

Consider the following standard state-space equations for an ASE module:

$$\dot{\mathbf{x}} = \mathbf{Ax} + \mathbf{Bu} + \boldsymbol{\Gamma}\boldsymbol{\eta}, \quad \mathbf{y} = \mathbf{Cx} + \mathbf{Du} + \boldsymbol{\Psi}\boldsymbol{\eta} \quad (1)$$

where $\mathbf{x} = (\mathbf{q}, \dot{\mathbf{q}}, \mathbf{q}_a, \mathbf{q}_\delta, \mathbf{q}_g)^T$ is the state vector and \mathbf{y} is the response vector.

The generalized-coordinate displacements $\mathbf{q}(t)$ associated with the subscripts a , δ , and g refer to the states due to aerodynamic lag, actuator dynamics, and gust filter dynamics, respectively. The vector \mathbf{u} is the actuator commanded input, and \mathbf{B} is the feedback control law relating the commanded control surface to the aircraft response. The parameter \mathbf{A} is the characteristic matrix of the aeroelastic system, \mathbf{C} is the sensor dynamics, $\boldsymbol{\Gamma}$ are the aerodynamic forces generated in response to a sinusoidal gust field, $\boldsymbol{\eta}$ is the white noise that yields the continuous gust spectrum, and \mathbf{D} and $\boldsymbol{\Psi}$ can arise due to aerodynamic lags.

Typically, Eq. (1) could result from the equation of motion that combines the finite element structure (e.g., ASTROS Structural Module) with linearized potential aerodynamics (e.g., ASTROS Aero Module), that is,

$$\bar{\mathbf{M}}\ddot{\mathbf{q}} + \bar{\mathbf{C}}\dot{\mathbf{q}} + \bar{\mathbf{K}}\mathbf{q} = \bar{\mathbf{Q}}(t) = \iint \boldsymbol{\Phi}^T \boldsymbol{\Delta} \mathbf{p}(t) dS \quad (2)$$

Presented as Paper 97-1181 at the AIAA/ASME/ASCE/AHS/ASC 38th Structures, Structural Dynamics and Materials Conference, Kissimmee, FL, 7–10 April 1997; received 19 June 1997; revision received 2 August 1999; accepted for publication 13 September 1999. Copyright © 1999 by the American Institute of Aeronautics and Astronautics, Inc. All rights reserved.

*Vice President.

†Member of Technical Staff.

‡Professor, Department of Mechanical and Aerospace Engineering. Associate Fellow AIAA.

§Associate Professor, Department of Aerospace Engineering. Associate Fellow AIAA.

where Φ is the structural modal matrix and \bar{M} , \bar{C} , and \bar{K} are the generalized mass, damping, and stiffness matrices of the system, respectively.

The actuator transfer function dynamics¹⁴ read

$$\dot{\mathbf{q}}_\delta = \mathbf{A}_\delta \mathbf{q}_\delta + \mathbf{B}_\delta \mathbf{u}, \quad \delta = \mathbf{C}_\delta \mathbf{q}_\delta \quad (3)$$

where δ are the control surface commanded deflections. \mathbf{A}_δ , \mathbf{B}_δ , and \mathbf{C}_δ are the dynamic matrix, the control distribution matrix, and the output matrix of the actuators, respectively.

The total generalized aerodynamic forces $\bar{\mathbf{Q}}(t)$ consist of three parts:

$$\bar{\mathbf{Q}}(t) = \mathbf{Q}\mathbf{q} + \mathbf{Q}_\delta\delta + \mathbf{Q}_g\mathbf{w}_g \quad (4)$$

where \mathbf{w}_g is the gust velocity vector, \mathbf{Q} is the generalized force matrix due to the aerodynamic forces resulting from the structural motion, \mathbf{Q}_δ is the generalized force matrix resulting from control surface deflections, and \mathbf{Q}_g is the generalized force matrix due to the gust pressure distribution. In the present ASE module, \mathbf{Q} , \mathbf{Q}_δ , and \mathbf{Q}_g will be recast from the k -domain aerodynamics into rational functions of s (i.e., the Laplace variable). The open loop of Eq. (1) can be closed via a gain matrix \mathbf{G} that relates \mathbf{u} to \mathbf{y} and that results in the closed-loop equation

$$\dot{\mathbf{x}} = \bar{\mathbf{A}}\mathbf{x} + \Gamma\mathbf{y} \quad (5)$$

where $\bar{\mathbf{A}} = \mathbf{A} + \mathbf{B} \cdot \mathbf{G} \cdot \mathbf{C}$.

State-space ASE models have been used in various applications of optimal (full-state feedback) and reduced-order control techniques such as those of Abel et al.¹⁶ and Mukhopadhyay et al.¹⁷ Clearly, recasting the equations of motion of the ASE system into the first-order, state-space form will allow the user of an MDO system such as ASTROS to apply various modern control techniques for control law design.

s-Domain Aerodynamics

Before the present effort,¹⁵ the earlier practice using ASTROS was to perform aeroelastic analysis for structural optimization in the frequency domain based on the linear subsonic/supersonic aerodynamics. For ASE practice, ASTROS is required to be supported by the *s*-domain aerodynamics. A unified *s*-domain aerodynamics (USDA) approach can be formulated using the unified unsteady (k -domain) aerodynamics of the ZAERO module in conjunction with the MIST method, as will be described. Thus, USDA will serve as the base of the ASE module. In this way, the capability of the developed ASTROS is enhanced to include the control and guidance discipline for a realistic aircraft, throughout its complete flight regime.

In a root-locus plot, the generalized aerodynamic forces \mathbf{Q} are normally available on the imaginary axis at a finite number of frequencies. Rather than using the cumbersome Laplace-transform technique, converting the frequency-dependent $\bar{\mathbf{Q}}(i\omega)$ to the time domain or complex s domain requires an approximation technique.^{10–14} Among existing methods MIST¹³ is selected here because it offers significant savings in the number of added states with little or no penalty in the accuracy of modeling the aerodynamic forces. The minimum-state approach converts $\bar{\mathbf{Q}}(i\omega)$ to $\bar{\mathbf{Q}}(s)$ in the following form:

$$\bar{\mathbf{Q}}(s) = \bar{\mathbf{A}}_0 + \bar{\mathbf{A}}_1(sb/V) + \bar{\mathbf{A}}_2(sb/V)^2 + \bar{\mathbf{D}}\bar{\mathbf{F}}(s)^{-1}\bar{\mathbf{E}}(sb/V) \quad (6)$$

where $\bar{\mathbf{F}}(s) = (sb/V)\mathbf{I} - \mathbf{R}$ and $\bar{\mathbf{A}}_i$ are the real-value approximation matrices, \mathbf{R} is a diagonal matrix with distinct negative terms representing the aerodynamic lags, and $\bar{\mathbf{D}}$ and $\bar{\mathbf{E}}$ are aerodynamic coupling matrices between the modal and aerodynamic states. With $\bar{\mathbf{Q}}(s)$ in hand, Eq. (2) along with Eq. (3) can be recast into a first-order, time-invariant, state-space form such as Eq. (1).

UAIC: ZAERO Module

The frequency-dependent generalized aerodynamic forces (GAF) $\bar{\mathbf{Q}}(i\omega)$ are obtained mainly from an aerodynamic influence coefficient- (AIC-) based aerodynamic method:

$$[\mathbf{Q}, \mathbf{Q}_\delta, \mathbf{Q}_g] =$$

$$q_\infty \Phi^T [\text{AIC}] \cdot \left\{ \frac{\partial \Phi}{\partial x} + i \frac{\omega}{V} \Phi, \frac{\partial \Phi_\delta}{\partial x} + i \frac{\omega}{V} \Phi_\delta, \exp \left[i \frac{\omega}{V} (x - x_g) \right] \right\} \quad (7)$$

where Φ_δ is the control surface displacement and the last exponential term is the downwash due to a sinusoidal gust field. The AIC matrix ordinarily relates the downwash to the aerodynamic forces on lifting surfaces. Earlier versions of the ASTROS aerodynamic module provide the [AIC] for lifting surfaces in subsonic flow (DLM¹⁸) and in supersonic flow (CPM¹⁹). No AICs in transonic or hypersonic flows nor any such AIC for wing-body configurations were available. Although recent advances in CFD methods have demonstrated their capability in computing unsteady aerodynamics for aeroelastic applications, they do not provide such AICs (for example, Refs. 20–23).

However, ASTROS and the present ASE module are formulated consistently with FEM and are normally solved by matrix-oriented methods. Without a major reformulation of the infrastructure of ASTROS, it would be difficult for ASTROS to adopt typical CFD solutions for aeroelastic applications.

Our effort in the past has been directed toward the construction of a unified approach in unsteady aerodynamic methods for all Mach numbers. This effort included the further development and validation of an unsteady transonic method (ZTAIC)^{7,24,25} and the generalization of the unsteady supersonic lifting surface method (ZONA51)^{4,26–28} to cover the unified hypersonic–supersonic ranges (ZONA51U).^{8,9}

The present UAIC approach is not confined to lifting surfaces; it also includes the wing–body unsteady subsonic/supersonic methods (ZONA6 and ZONA7).^{5,6,27}

Results and Discussion

National Aerospace Plane (NASP) Demonstrator Wing²⁹

The NASP demonstrator wing is a cropped delta planform with a hexagon profile wing cross section (Fig. 1).

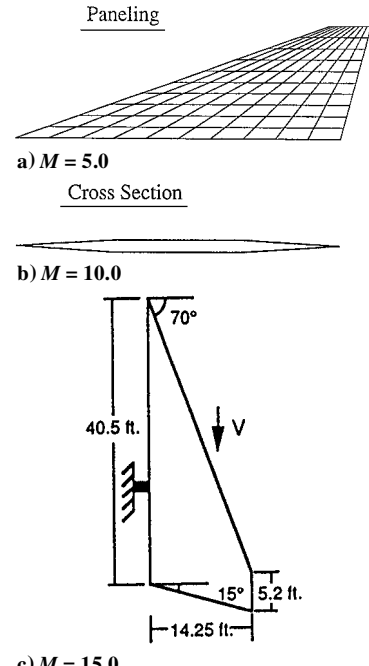


Fig. 1 NASP demonstrator wing: a) aerodynamic model, b) cross section, and c) dimensions.

Table 1 Comparison of flutter dynamic pressures and frequencies of NASP demonstrator model at $M = 5.0, 10.0$, and 15.0

Aerodynamic method	Mach number								
	5			10			15		
	q_f , psi	ω_f , r/s	h , ^a kft	q_f , psi	ω_f , r/s	h , ^a kft	q_f , psi	ω_f , r/s	h , ^a kft
Piston theory	129	78	18	184	78	42	250	72	51
QSCFD, two dimensional	169	80	11	331	81	28	982	224	22
QSCFD, three dimensional	—	—	—	330	82	28	981	224	22
ZONA51U									
$V-g$ method	129	82	18	175	73	42	206	70	55
s -domain	130	82	18	184	71	41	213	68	54

^a Approximate matchpoint altitude.

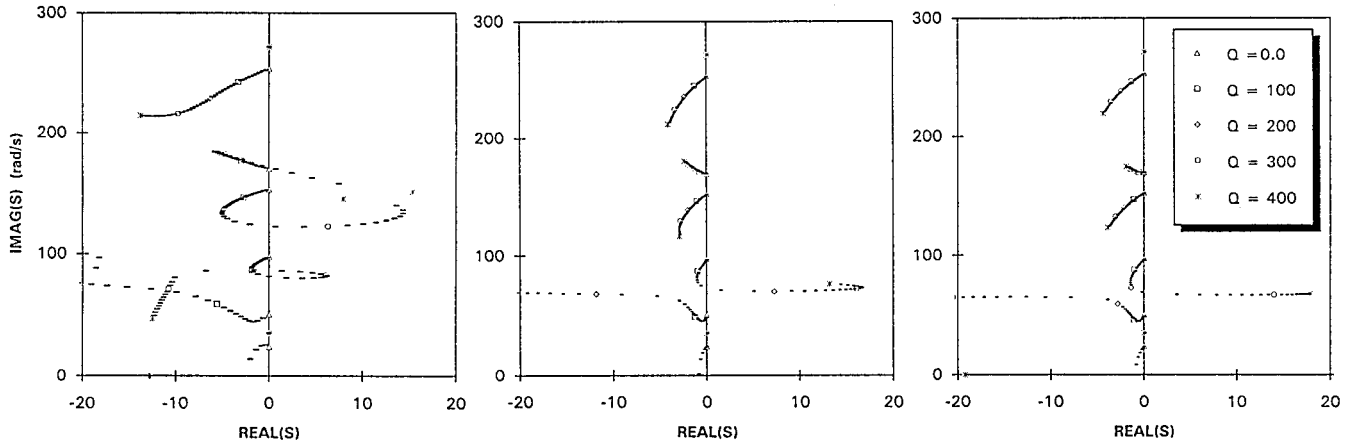


Fig. 2 Root-locus plots of NASP demonstrator model at $M = 5.0, 10.0$, and 15.0 (Q = dynamic pressure).

Figure 2 presents the root-locus plot at three Mach numbers based on eight modes. For cases at $M_\infty = 5.0, 10.0$, and 15.0 , mode 4 is found to flutter at dynamic pressures q_f at 130, 184, and 213 psi, respectively.

Extensive comparison of various computed results has been carried out in the present NASP wing case. In Table 1, the flutter results of ZONA51U using the $V-g$ method and using the root-locus method are compared with those of Piston theory and the NASA CFD codes (QSCFD2d and 3d).³⁰ Several observations can be made with respect to the collected data.

1) Good agreement is found between the flutter q of the $V-g$ method and the root-locus method based on ZONA51U. Flutter frequencies are also found to agree well.

2) Piston theory results follow the general trend predicted by ZONA51U, except that the former results tend to be overestimated at high Mach numbers.

3) Substantial discrepancies are found between the NASA/CFD results and the ZONA51U results: ZONA51U predicts more conservative flutter speeds at higher altitudes, whereas the NASA/CFD codes predict less conservative speeds at lower altitudes. In fact, ZONA51U gives the most conservative answers for all cases in this study.

Modeled F-16 Wing³¹

Figure 3 shows the aerodynamic/structural model and the flutter boundary of a modeled F-16 wing. The wing planform has an aspect ratio of 2.8, with 4% thick parabolic arc airfoil sections. The flutter speeds and frequencies are computed by the $V-g$ method at six Mach numbers $M_\infty = 0.7, 0.75, 0.8, 0.85, 0.9$, and 0.95 . It is seen that the flutter results of ZTAIC are in good agreement with those of XTRAN3S²¹ and CAP-TSD,²² especially at $M_\infty = 0.95$. Notice that the flutter (modal) mechanism changes from $M_\infty = 0.9$ to 0.95 , as indicated by the jump in the flutter frequency (from 6.8 to 19 Hz). ZTAIC concurs with the other two codes in the prediction of this mechanism.

Figure 4 presents the s -domain results by MIST for four GAFs. For this case, MIST achieves a better fit than that for the case of the 445.6 wing (Fig. 5). Notice that the dotted lines in the background are the fitted subsonic GAFs using ZONA6. Substantial differences can be seen between the results of ZTAIC and ZONA6, showing strong transonic characteristics of this wing at $M_\infty = 0.95$.

AGARD Standard 445.6 Wing³²

The 445.6 wing is a swept tapered planform with an aspect ratio of 4 and a NACA 65A004 airfoil section. It has two structural models: the solid wing and the weakened wing. This is an ideal case to demonstrate ZTAIC's AIC capability. The aerodynamic shapes of these two models remain the same, but structurally they should have two different sets of baseline modes. However, these two sets of modes are subject to the same structural boundary conditions. For this reason, the same modal AIC can be shared by both models. Hence, the modal AIC computed for the weakened wing can be saved allowing for a warm-start for the solid wing. Table 2 presents the flutter results of the weakened and solid wings. At a subsonic Mach number $M_\infty = 0.678$, the ZTAIC result is in good agreement with that of ZONA6, as expected. At other supercritical Mach numbers, where $M_\infty = 0.9$ and 0.95 , ZTAIC predicts a pronounced transonic dip that is comparable to that predicted by the CAP-TSD code.^{22,23}

Figure 5 presents the s -domain results by MIST for the GAFs of the 445.6 weakened wing at $M_\infty = 0.95$. Unlike the preceding cases for the F-16 wing, some slight discrepancy is found in the GAF (1, 2), which might be caused by the stringent feature of the supercritical mean flow at this Mach number.

Figure 6 presents the root-locus plot of the same case using the preceding MIST results. The flutter speed predicted here ($V_f = 1015$ fps) is in reasonable agreement with the one predicted by the $V-g$ method ($V_f = 944$ fps, see Table 2). The discrepancy is perhaps caused by the slight inaccuracy from the MIST approximation in the transonic range.

Table 2 Weakened and solid model 445.6 wing flutter results

Test cases		Wind-tunnel data		ZONA6 - - - (linear)		ZTAIC Δ (nonlinear)		CAPTSD \diamond (nonlinear)	
M	ρ , slug/ft ³	ω_f , Hz	V_f , ft/s	ω_f , Hz	V_f , ft/s	ω_f , Hz	V_f , ft/s	ω_f , Hz	V_f , ft/s
<i>Weakened Wing Model</i>									
0.678	0.000404	17.98	759.1	19.81	766.0	19.30	761.0	19.2	768
0.900	0.000193	16.09	973.4	16.31	984.0	16.38	965.2	15.8	952
0.950	0.000123	14.50	1008.4	16.18	1192.0	13.46	944.0	12.8	956
<i>Solid Wing Model</i>									
0.90	0.00357	27.00 ^a	452.0 ^a	26.75	439.0	25.71 ^b	418.0 ^b	25.8 ^a	435.0 ^a
0.95	0.00320	26.91 ^a	479.0 ^a	26.89	462.0	25.46 ^b	450.0 ^b	26.2 ^a	472.1 ^a

^aInterpolated between Mach 0.87, 0.92, and 0.96. ^bRestart run using AIC's of weakened wing (1 min CPU/case).

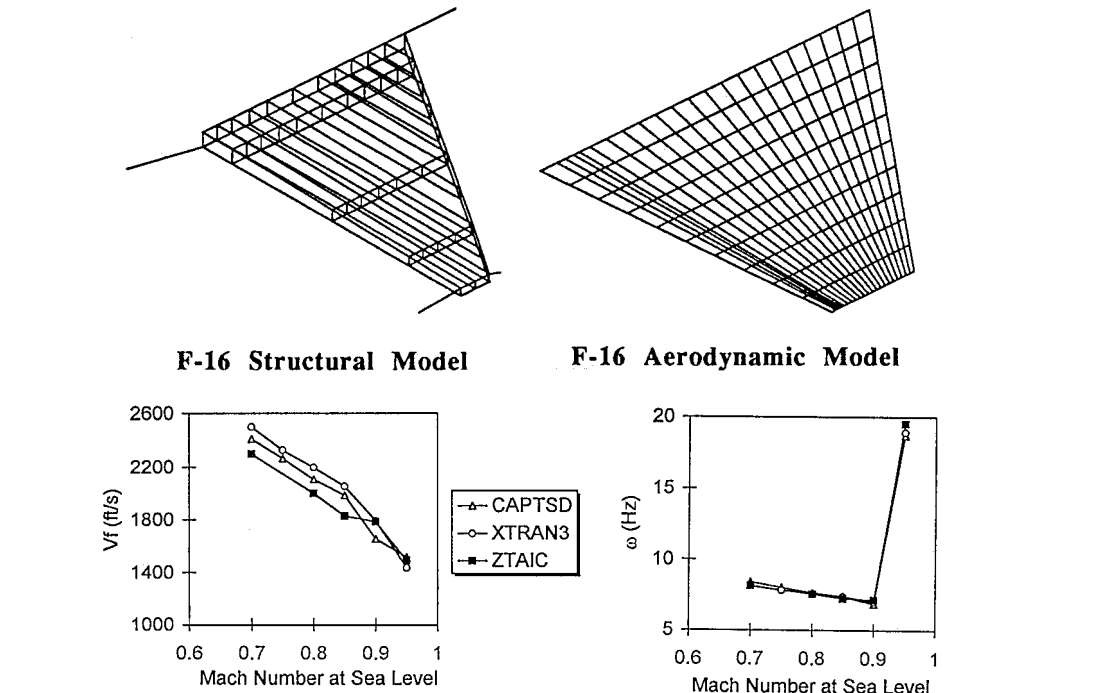


Fig. 3 Flutter speeds and frequencies of modeled F-16 wing computed by ZTAIC, CAPTSD, and XTRAN3.

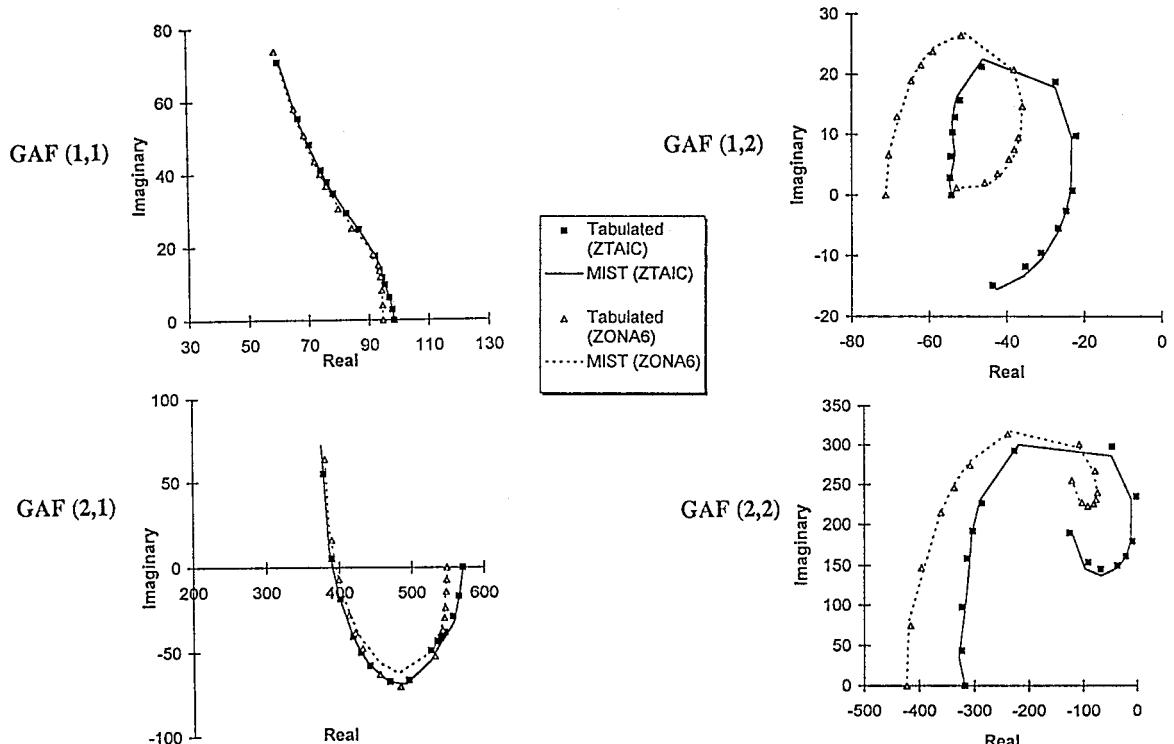


Fig. 4 Minimum-state approximation of GAF of modeled F-16 wing at $M = 0.95$ computed by ZTAIC and ZONA6.

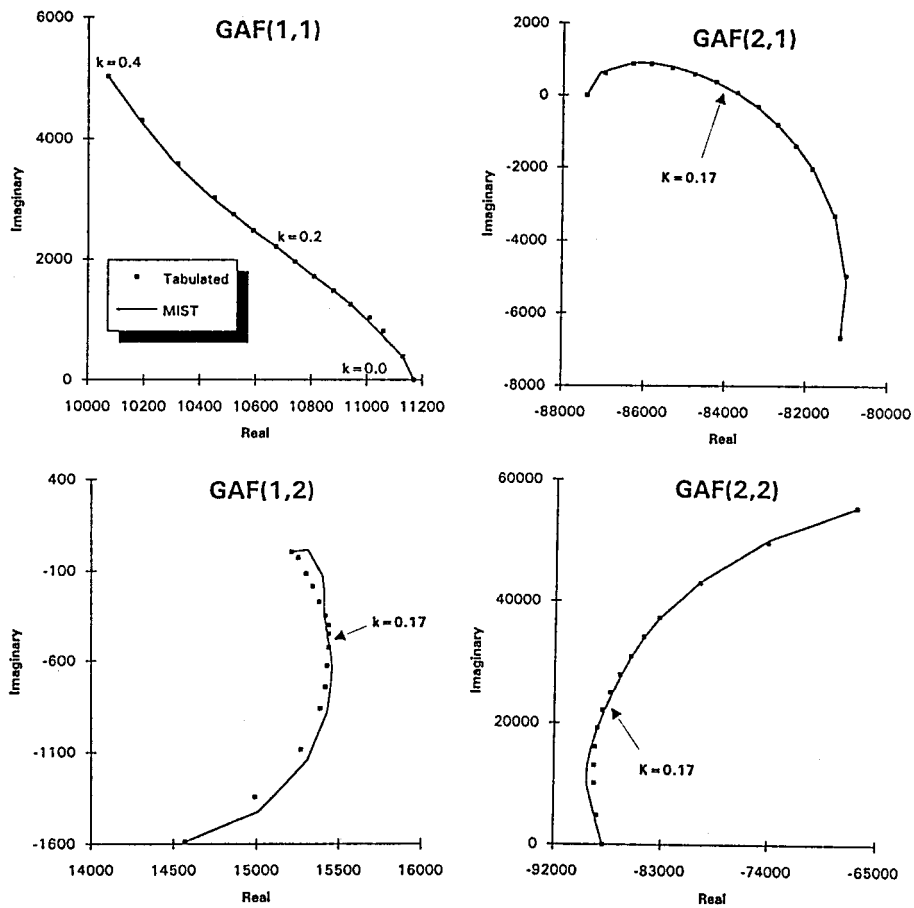


Fig. 5 Minimum-state approximation of GAF of 445.6 weakened wing at $M = 0.95$ computed by ZTAIC.

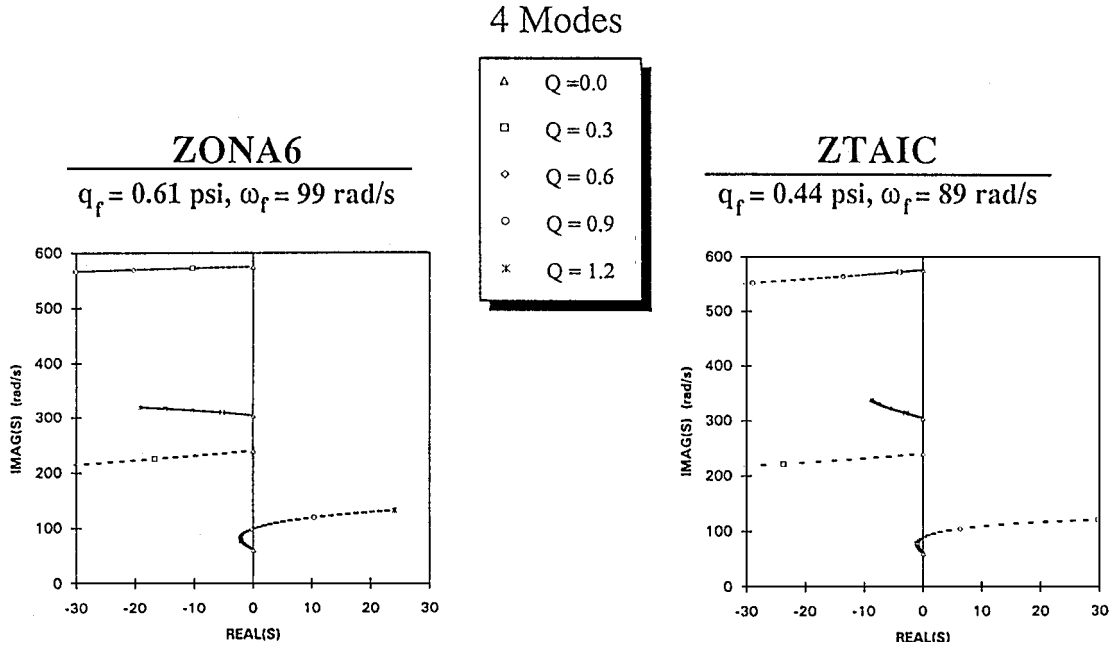


Fig. 6 Root-locus plots of 445.6 weakened wing at $M = 0.95$ using s -domain aerodynamics computed by ZTAIC and ZONA6.

Conclusions

The development of a unified aerodynamics module ZAERO and the ASE module and our current effort in their integration to ASTROS are presented. A unified AIC approach has been firmly established that is fully compatible with structural FEM and, hence, with ASTROS. Based on this unified AIC approach, both modules can be used for aeroelastic/ASE analysis and MDO applications. The UAIC approach extends our current wing-body AIC

method from the linear flow regimes to the transonic and unified hypersonic-supersonic regimes. Hence, it renders the ZAERO module applicable to all Mach numbers and in the full range of the k domain.

By means of the MIST method, the k -domain aerodynamics of ZAERO can be effectively converted into the s -domain aerodynamics, which is readily adaptable by the ASE module and other control practice.

Cases studied of three different wing planforms show that MIST is an effective and accurate method for s -domain solutions in all flight regimes, including the transonic and hypersonic regimes.

Acknowledgments

The present work is supported in part by the AF/STTR Phase I/II Contract F33615-96-C3217. The technical advice and assistance received from Gerald Anderson, Ray Kolonay, Vipperla B. Venkayya, Ed Pendleton, and Larry Huttell of the U.S. Air Force Research Laboratory are gratefully acknowledged.

References

- ¹Johnson, E. H., and Venkayya, V. B., "Automated Structural Optimization System (ASTROS), Theoretical Manual," U.S. Air Force Research Lab., TR-88-3028, Vol. 1, Wright-Patterson AFB, OH, Dec. 1988.
- ²Thomas, J. L., Taylor, S. L., and Anderson, W. K., "Navier-Stokes Computations of Vortical Flows over Low Aspect Ratio Wings," AIAA Paper 87-0207, Jan. 1987.
- ³Guruswamy, G. P., "Time-Accurate Unsteady Aerodynamic and Aeroelastic Calculations of Wings Using Euler Equations," AIAA Paper 88-2281, April 1988.
- ⁴Chen, P. C., and Liu, D. D., "A Harmonic Gradient Method for Unsteady Supersonic Flow Calculations," *Journal of Aircraft*, Vol. 22, No. 5, 1985, pp. 371-379.
- ⁵Chen, P. C., and Liu, D. D., "Unsteady Supersonic Computation of Arbitrary Wing-Body Configurations Including External Stores," *Journal of Aircraft*, Vol. 27, No. 2, 1990, pp. 108-116.
- ⁶Chen, P. C., Lee, H. W., and Liu, D. D., "Unsteady Subsonic Aerodynamics for Bodies and Wings with External Stores Including Wake Effort," *Journal of Aircraft*, Vol. 30, No. 5, 1993, pp. 618-628.
- ⁷Chen, P. C., Sarhaddi, D., and Liu, D. D., "Transonic AIC Approach for Aeroelastic and MDO Applications," Euromech Colloquium 349, Göttingen, Germany, Sept. 1996 (to be published).
- ⁸Liu, D. D., Chen, P. C., Yao, Z. X., and Sarhaddi, D., "Recent Advances in Lifting Surface Methods," *Aeronautical Journal*, Vol. 100, No. 998, 1996, pp. 327-339.
- ⁹Liu, D. D., Yao, Z. X., Sarhaddi, D., and Chavez, F., "From Piston Theory to a Unified Hypersonic-Supersonic Lifting Surface Method," *Journal of Aircraft* (to be published); also International Council of the Aerospace Sciences, Paper 94-2.8.4, 1994.
- ¹⁰Roger, K. L., "Airplane Math Modeling Methods for Active Control Design," *Structural Aspects of Active Controls*, CP-228, AGARD, 1977, pp. 4-1-4-11.
- ¹¹Adams, W. M., Jr., and Hoadley, S. T., "ISAC: A Tool for Aeroelastic Modeling and Analysis," AIAA Paper 93-1421-CP, April 1993.
- ¹²Vepa, R., "Finite State Modeling of Aeroelastic Systems," NASA CR-2779, 1977.
- ¹³Karpel, M., "Time-Domain Aeroservoelastic Modeling Using Weighted Unsteady Aerodynamic Forces," *Journal of Guidance, Control, and Dynamics*, Vol. 13, No. 1, 1990, pp. 30-37.
- ¹⁴Karpel, M., and Strull, E., "Minimum-State Unsteady Aerodynamic Approximation with Flexible Constraints," *International Forum on Aeroelasticity and Structural Dynamics*, Royal Aeronautical Society, London, 1995, pp. 66.1-66.8.
- ¹⁵ZONA, OU, Karpel, UAI, "Enhancement of the Aeroservoelastic Capability in ASTROS," WLTR-96-3119, STTR Phase I Final Report, Sept. 1996.
- ¹⁶Abel, I., Newsom, J. R., and Dunn, H. J., "Application of Two Synthesis Methods for Active Flutter Suppression on an Aeroelastic Wind-Tunnel Model," A Collection of TP-AIAA Atmospheric Flight Mechanics Conference for Future Space Systems, Aug. 1979, pp. 93-107.
- ¹⁷Mukhopadhyay, V., Newsom, J. R., and Abel, I., "A Method for Obtaining Reduced-Order Control Laws for High-Order Systems Using Optimization Techniques," NASA TP 1876, Aug. 1981.
- ¹⁸Rodden, W. P., Giesing, J. P., and Kalman, T. P., "New Developments and Applications of the Subsonic Doublet Lattice Methods for Non-Planar Configurations," CP-80-71, AGARD, Pt. 2, No. 4, 1971.
- ¹⁹Appa, K., "Constant Pressure Panel Method for Supersonic Unsteady Airloads Analysis," *Journal of Aircraft*, Vol. 24, No. 10, 1987, pp. 696-702.
- ²⁰Lee-Rausch, E. M., and Batina, J. T., "Wing Flutter Boundary Prediction Using Unsteady Euler Aerodynamic Method," AIAA Paper 93-1422, April 1993.
- ²¹Borland, C. J., and Sotomayer, W. A., "An Algorithm for Unsteady Transonic Flow About Tapered Wings," AIAA Paper 84-1567, 1984.
- ²²Batina, J. T., "An Efficient Algorithm for Solution of the Unsteady Transonic Small Disturbance Equation," *Journal of Aircraft*, Vol. 25, No. 7, 1988, pp. 598-605; also NASA TM 89014, Dec. 1986.
- ²³Bennett, R. M., Batina, J. T., and Cunningham, H. J., "Wing-Flutter Calculations with the CAP-TSD Unsteady Transonic Small-Disturbance Program," *Journal of Aircraft*, Vol. 26, No. 9, 1989, pp. 876-882.
- ²⁴Liu, D. D., Kao, Y. F., and Fung, K. Y., "An Efficient Method for Computing Unsteady Transonic Aerodynamics of Swept Wings with Control Surfaces," *Journal of Aircraft*, Vol. 25, No. 1, 1988, pp. 25-31; also AIAA Paper 85-4058, 1985.
- ²⁵Chen, P. C., Yao, Z. X., and Liu, D. D., "A New AIC Development of ZONA6/ZONA7 Codes for Applications to Advanced Aircraft Configurations," ZONA 91-17A, Sept. 1992.
- ²⁶Liu, D. D., James, D., Chen, P. C., and Pototsky, A., "Further Studies of Harmonic Gradient Method for Supersonic Aeroelastic Applications," *Journal of Aircraft*, Vol. 28, No. 9, 1991, pp. 598-605.
- ²⁷Chen, P. C., Yao, Z. X., and Liu, D. D., "An Analysis in the AIC Formulation for Wing-Body Configurations," ZONA6/ZONA7 Supplement Series A, ZONA Technology, Inc., ZONA91-17, Scottsdale, AZ, June 1991.
- ²⁸Johnson, E. H., Rodden, W. P., Chen, P. C., and Liu, D. D., "Comments on 'Canard-Wing Interaction in Unsteady Supersonic Flow,'" *Journal of Aircraft*, Vol. 29, No. 4, 1992, p. 744.
- ²⁹Scott, R. C., and Pototsky, A. S., "A Method of Predicting Quasi-Steady Aerodynamics for Flutter Analysis of High Speed Vehicles Using Steady CFD Calculations," AIAA Paper 93-1364, April 1993.
- ³⁰Walters, R., Reu, T., McGrory, W., and Richardson, P., "A Longitudinally-Patched Grid Approach with Applications to High Speed Flows," AIAA Paper 88-0715, Jan. 1988.
- ³¹Kolonay, R., "Unsteady Aeroelastic Optimization in the Transonic Regime," AIAA 96-3983-CP, 6th AIAA/NASA/ISSMO Symposium on MAO, Pt. 1, Bellevue, WA, Sept. 1996.
- ³²Yates, E. C., Jr., Land, N. S., and Foughner, J., Jr., "Measured and Calculated Subsonic and Transonic Flutter Characteristics of a 45 Deg Sweptback Wing Planform in Air and in Freon-12 in the Langley Transonic Dynamics Tunnel," NASA TN D-1616, March 1963.